

Search for the Flavor-Changing Neutral-Current Decay $\Sigma^+ \rightarrow p\mu^+\mu^-$

HyangKyu Park ^a

^aUniversity of Michigan, Ann Arbor, Michigan 48109, USA
(For the HyperCP Collaboration)

The Fermilab HyperCP (E871) experiment collected on the order of 10^{10} hyperon decays. Based on an analysis of the entire data set, we will report on the observation of events with reconstructed masses consistent with that of Σ^+ assuming the final state $p\mu^+\mu^-$. If the observed events are the decay $\Sigma^+ \rightarrow p\mu^+\mu^-$, then they would be the first evidence of this decay. Other possible interpretations of the observed events will also be discussed.

1. Introduction

In the standard model (SM), the decay $\Sigma^+ \rightarrow pl^+l^-$ (Σ_{pl}^+ , $l = e, \mu$) occurs via the flavor-changing neutral-current (FCNC) interaction and the internal conversion, as shown in Fig. 1 (a)-(c). It was argued that the FCNC contribution for the decay Σ_{pl}^+ within the SM is not a dominant one [2]. The decay Σ_{pl}^+ also serves as a search for a new light scalar or vector particle, which could mimic the FCNC interaction [1] (see Fig. 1 (d)).

There is only an upper limit for $B(\Sigma^+ \rightarrow pe^+e^-) < 7 \times 10^{-6}$ [3]. The decay rate for the process $\Sigma^+ \rightarrow pl^+l^-$ was calculated in [2,4] using experimental partial decay width and decay parameter of $\Sigma^+ \rightarrow p\gamma$ decays. In [2], the possible ranges for the ratio of the decay rates within the SM were obtained: $1/1210 \lesssim \Gamma(\Sigma^+ \rightarrow p\mu^+\mu^-)/\Gamma(\Sigma^+ \rightarrow pe^+e^-) \lesssim 1/120$, which give a good test of the SM in these modes. Any violation of these limits would be a signal of new physics.

2. The HyperCP Experiment

The HyperCP experiment (E871) at Fermilab collected data during the 1997 and the 1999 runs. The experiment was designed to investigate CP violation and to study rare decays of hyperons and kaons. The spectrometer is described in detail elsewhere [5], and a plan view of the spectrometer is shown in Fig. 2. A charged secondary beam was produced by directing an 800 GeV pro-

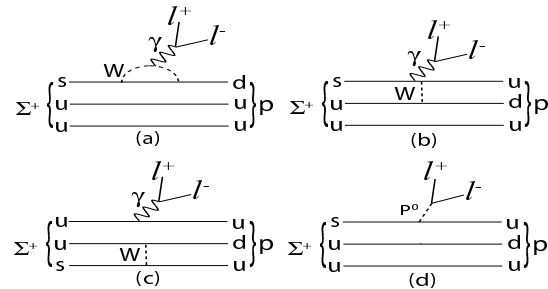


Figure 1. Feynman diagrams for Σ_{pl}^+ decays in SM and a new physics. (a)-(c) SM processes, FCNC and internal conversion respectively. (d) A new particle P^0 contribution.

ton beam onto a 2×2 mm² copper target. The momenta of secondaries and their charges were selected by a curved collimator channel embedded in a 6 m-long dipole magnet (Hyperon Magnet) set to an average momentum of 160 GeV/c.

Most of hyperons exiting from the collimator decayed inside a 13 m-long vacuum decay pipe. After the decay pipe, the decay products were detected in nine multi-wire proportional chambers (C1-C9). There are two scintillation hodoscopes, which are the basis for most of the physics trigger. Two muon stations are placed on either side of the beam line. Each station consisted of three layers of steel blocks and proportional-wire tubes. At the middle and rear of each station were two

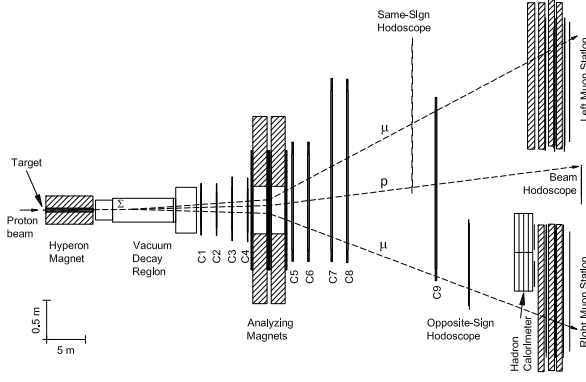


Figure 2. Plan view of the HyperCP spectrometer.

hodoscopes for triggering on muons.

The polarities of both the Hyperon and Analyzing magnets were periodically reversed to select either positively or negatively charged secondaries.

3. Analysis

We searched for $\Sigma_{p\mu\mu}^+$ decays using the data set collected during the 1997 and 1999 runs. The event topology for $\Sigma_{p\mu\mu}^+$ decays is three tracks coming from a single vertex. Two muon tracks tagged by both left- and right-side muon detectors and one proton track in the left side with respect to the secondary beam line were required.

The basic selection cut was designed for rejection of most backgrounds that were mainly produced at the exit of the collimator. The total momentum of the three tracks had to be within the expected range of 120 and 240 GeV/c. The Σ^+ had to originate at the x and y positions of the target within 3.5 mm. The z position of the decay vertex estimated by the method of distance of closest approach was required to be between 100 cm and 1300 cm from the exit of the collimator. Events with a single vertex were selected by fitting three tracks to a common vertex and requiring the average transverse distance at the z -coordinate of the vertex of the event to be <

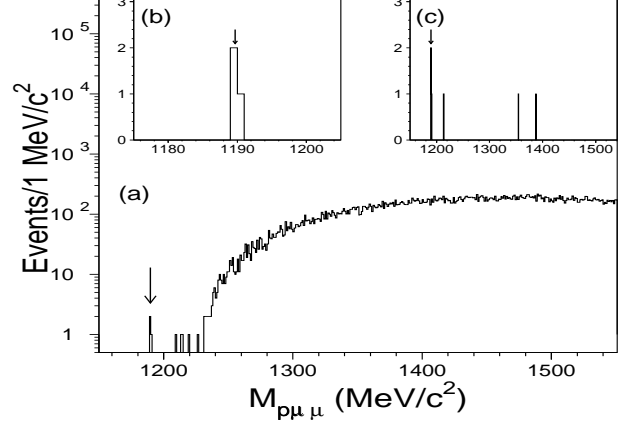


Figure 3. Mass distributions with $\Sigma_{p\mu\mu}^+$ decay hypothesis for the positive-secondary-beam data, (a) after the standard cuts, (b) within $\pm 15 \sigma$ of the mass resolution at the Σ^+ mass, and (c) after the extended cuts. The arrow represents the Σ^+ mass.

2.5 mm. The χ^2/ndf of the fit was required to be less than 1.5.

For events passing the cuts, we reconstructed the invariant mass ($M_{p\mu\mu}$). The MC study shows that the mass resolution for $\Sigma^+ \rightarrow p\mu^+\mu^-$ decay in the HyperCP spectrometer is 1.0 MeV/c². Three candidates were observed only in the positive-secondary beam data with masses within 1 σ of the Σ^+ mass. There are no background events within $\approx 20 \sigma$ of the Σ^+ mass. The mass distributions are shown in Fig. 3 (a) and (b).

As a further check, the candidates were verified by applying extended cuts to the sample in Fig 3 (a); these removed most of charged kaon backgrounds. In the extended cuts, the ratio of proton momentum to the sum of three track momentum (f_{pro}) was required to be larger than 0.68. Events were also eliminated if the mass reconstructed as $K^+ \rightarrow \pi^+\mu^+\mu^-$ ($K_{\pi\mu\mu}$) decays was within ± 10 MeV/c² at the K^+ mass. After the extended cuts, the signals of the three candidates are very clean, as shown in Fig 3 (c).

MC simulations were used to check on the possible background such as charged kaon decays and

muon pair production by photon conversion in material inside the vacuum decay pipe. We typically generated 100 times more MC events for each background source than the expected background level. In order to investigate possible backgrounds we missed, we used the real data, unlike-signed dimuon sample for the negative-secondary-beam data as well as the single muon sample for both positive- and negative-secondary-beam data. The background studies showed that none of the background sources after the cut contributed in the invariant mass region below 1200 MeV/c^2 . Finally, we relaxed each cut value to increase the background level in Fig 3 (c) by an order of magnitude. However, there was still no background event within 8σ . Based on the background studies, the three candidates are unlikely due to background.

In the measurement of the branching ratio for $\Sigma_{p\mu\mu}^+$ decays, the decay $\Sigma^+ \rightarrow p\pi^0, \pi^0 \rightarrow ee\gamma$ ($\Sigma_{pee\gamma}^+$) was used for the normalization mode. The basic selection and f_{pro} cut values required for $\Sigma_{pee\gamma}^+$ decay were optimized by MC simulation of this decay. In order to reduce photon conversion events, the invariant mass for two electrons was required to be between 50 MeV/c^2 and 100 MeV/c^2 , and the decay vertex had to be 200 $\text{cm} < v_z < 1300 \text{ cm}$ to reject background from the upstream vacuum window. After the selection criteria for $\Sigma_{pee\gamma}^+$ decays, a total of 211 events were left as shown in Fig. 4. From the fit, the number of observed $\Sigma_{pee\gamma}^+$ decays was $N_{nor}^{obs} = (193.5 \pm 27.9)$ events, where the uncertainty is statistical only.

4. Interpretations of Results

The reconstructed dimuon masses for the three events were 214.7 MeV/c^2 , 214.3 MeV/c^2 and 213.7 MeV/c^2 , which are within the expected dimuon mass resolution ($\sigma \approx 0.5 \text{ MeV}/c^2$). The dimuon mass ($M_{\mu\mu}$) for the three events is compared with the dimuon mass distribution expected for 3-body decay $\Sigma^+ \rightarrow p\mu^+\mu^-$ in Fig. 5 (a), where the decay model with form factors is explained below. Several interpretations are possible for the unexpectedly narrow dimuon mass distribution. The results presented here are very preliminary.

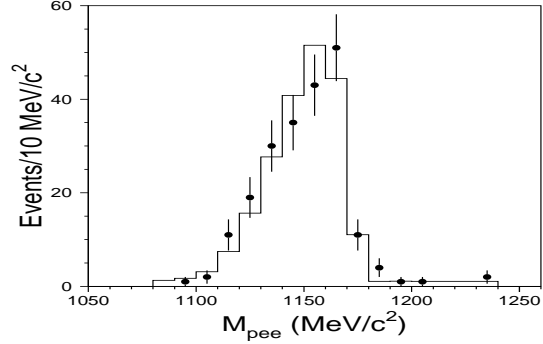


Figure 4. The reconstructed mass pe^+e^- for the normalization mode after all cuts. The histogram is the sum of MC samples, where each MC composition was determined by the fit, and the MC histogram was normalized to the observed data events. The solid points are for the data.

First, we assume the three candidates are direct $\Sigma^+ \rightarrow p\mu^+\mu^-$ decays and estimate the branching ratio of this decay. In order to measure the branching ratio, we estimated the acceptances using two decay models, a uniform phase space decay (Model A) and a form factor (Model B) [2]. Model B used the SM processes, FCNC as well as the internal conversion diagrams, as shown in Fig. 1 (a)-(c), and some of the form factor functions for hadronic matrix element were extracted from the experimental data for $\Sigma^+ \rightarrow p\gamma$ decays. MC simulations were used to estimate the geometric acceptances and the event-selection efficiencies for the signal and normalization modes. Table 1 shows a summary of the results. The systematic error in the measurement of the branching ratio was dominated by the modeling of the Σ^+ production. The estimated branching ratios for $\Sigma_{p\mu\mu}^+$ decays with the decay models, Model A and Model B, are found to be $[1.3^{+1.0}_{-0.8}(stat) \pm 0.7(syst)] \times 10^{-7}$ and $[8.6^{+6.6}_{-5.4}(stat) \pm 5.0(syst)] \times 10^{-8}$, respectively.

If the three candidates are unknown background, the upper limit of $B(\Sigma_{p\mu\mu}^+) < 1.6 \times 10^{-7}$ (1.1×10^{-7}) for Model A (B) at 90 % C.L. is obtained since we found no events at $M_{\mu\mu} > 215$

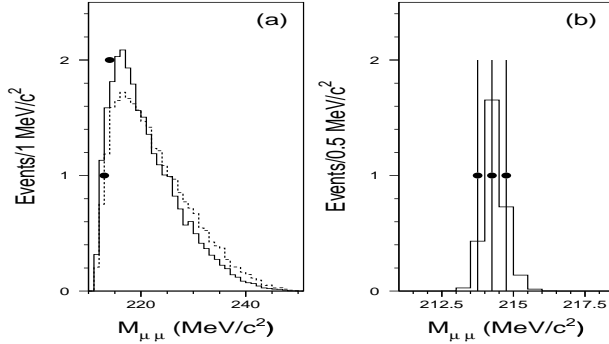


Figure 5. $M_{\mu\mu}$ distributions; (a) MC events with an arbitrary normalization for $\Sigma^+_{p\mu\mu}$ decays with uniform phase space decay (dotted histogram) and the form factor model (histogram), and (b) MC events (histogram) for $\Sigma^+ \rightarrow pP^0, P^0 \rightarrow \mu^+\mu^-$ decays. The solid points represent the data.

MeV/c^2 .

Since the dimuon masses for the three events are clustered within $\approx 1 \text{ MeV}/c^2$, they may not be due to $\Sigma^+ \rightarrow p\mu^+\mu^-$ decays. A MC, which produces the dimuon mass distribution in Fig. 5 (a) for the three-body $\Sigma^+_{p\mu\mu}$ decays with Model A and B, was used to estimate the probability for the dimuon masses for a three events to be within $1 \text{ MeV}/c^2$ anywhere within the kinematic range of the dimuon mass. This probability was found to be less than 1% for both Model A and B, which suggests a two-body decay $\Sigma^+ \rightarrow pP^0, P^0 \rightarrow \mu^+\mu^-$ ($\Sigma^+_{pP^0\mu\mu}$), where P^0 is an unknown particle with the mass $(214.3 \pm 0.5) \text{ MeV}/c^2$. The dimuon mass distribution for the three candidates is compared with MC events for $\Sigma^+_{pP^0\mu\mu}$ decays in Fig. 5 (b), and a good agreement is found. In the case of the hypothesis of $\Sigma^+_{pP^0\mu\mu}$ decays, the branching ratio was estimated as $B(\Sigma^+ \rightarrow pP^0, P^0 \rightarrow \mu^+\mu^-) = (3.1^{+2.4}_{-1.9}(\text{stat}) \pm 1.5(\text{syst})) \times 10^{-8}$. This would be consistent with the pseudoscalar sgoldstino suggested by Gorbunov and Rubakov [1].

5. Summary

We observed three candidates with $p\mu\mu$ mass consistent with the Σ^+ mass. If they are $\Sigma^+ \rightarrow p\mu^+\mu^-$ decays, this is the first observation of this decay. The three candidates were also consistent with the hypothesis, $\Sigma^+ \rightarrow pP^0, P^0 \rightarrow \mu^+\mu^-$ decays, which leads to the possible observation of a new particle, P^0 , with a mass $(214.3 \pm 0.5) \text{ MeV}/c^2$. Further work is needed to confirm this result.

6. Acknowledgments

Thanks to the conference organizers for a very enjoyable and fruitful meeting. We are indebted to the staffs of Fermilab and the HyperCP collaborators for their vital contributions. This work was supported by the U.S. Department of Energy and the National Science Council of Taiwan, R.O.C.

Table 1

Summary of the estimated acceptances (A_i) and efficiencies (ϵ_i) for the signal and normalization modes. The cut efficiency after the cut $M_{\mu\mu} > 215 \text{ MeV}/c^2$ is in parenthesis.

Mode	A_i (%)	ϵ_i (%)
Model A for $\Sigma^+_{p\mu\mu}$ decays	0.168	71.0 (61.2)
Model B for $\Sigma^+_{p\mu\mu}$ decays	0.259	71.2 (58.4)
$\Sigma^+_{pP^0\mu\mu}$ decays	0.731	69.1
Normalization	0.255	5.62

REFERENCES

1. D.S. Gorbunov and V.A. Rubakov, Phys. Rev. D **64**, 054008 (2001).
2. L. Bergström, R. Safadi and P. Singer, Z. Phys. C **37**, 281 (1988).
3. Particle Data Group, S. Eidelman *et al.*, Phys. Lett. B **592** (2004).
4. Dennis Corrigan and N.N. Trofimenkoff, Nucl. Phys. B **40**, 98 (1971).
5. R. A. Burnstein *et al.*, submitted to Nucl. Instrum. Methods; hep-ex/0405034.